http://www.scirp.org/journal/ns Natural Science, 2019, Vol. 11, (No. 8), pp: 257-266

Potential Power of the Pyramidal Structure

Osamu Takagi[1], Masamichi Sakamoto[2], Hideo Yoichi[1], Kimiko Kawano[1], Mikio Yamamoto[1]

[1]International Research Institute (IRI), Inage, Chiba, Japan; [2]Aquavision Academy, Narita, Chiba, Japan

Correspondence to: Osamu Takagi, takagi@a-iri.org

Keywords: Pyramid, Potential Power, Meditation, Unconsciousness, Non-Contact Effect, Delay, Biosensor, Cucumber, Gas

Received: July 24, 2019 **Accepted:** August 26, 2019 **Published:** August 29, 2019

ABSTRACT

There have been various traditions and books which describe a so-called "pyramid power", but there have been almost no reliable academic studies and no statistically significant data about it. We have continued scientifically rigorous experiments using biosensors to elucidate unexplained functions of a pyramidal structure (PS) since 2007. We used edible cucumber sections as biosensors and measured the concentrations of gas emitted from the sections by a technique developed by our group. From them we have demonstrated with high statistical accuracy the existence of the "pyramid power", which was often recognized as having no scientific basis. We reached two conclusions from the work. 1) The PS converted the unconsciousness of a human (the test subject) more than 6 km away to energy detectable by the biosensors (1% significance). 2) The PS accumulated the influence that a human (the test subject) had when meditating within the PS. Then the PS converted the influence into the energy detectable by the biosensors (10^{-3}% significance). These two conclusions showed that the functions of the PS were detected when "the PS and a human were related". On the other hand, we hypothesized that the potential power of the PS could be detected even when "the PS and a human were not related". In this paper, our purpose is to verify the existence of the potential power of the PS alone by experiment when "the PS and a human were not related". The following three results were obtained by experiment. 1) The presence of the potential power of the PS was demonstrated with 1% significance. 2) The potential power of the PS changed in value between summer and winter, and it was clear that the non-contact effect on the biosensors was larger in summer and smaller in winter. 3) The potential power of the PS affected only the biosensors placed at the PS apex, and did not affect the biosensors placed at the calibration control point 8 m away from the PS. This paper is the first report in the world to show this type of effect by scientific measurements. Our research results may open up a new science field of "pyramid power", from which we

expect further development of fields applying this "pyramid power".

1. INTRODUCTION

Unexplained functions which a pyramidal structure (PS) is said to have are of great interest. And there have been various traditions and books which describe these functions, there have been almost no reliable academic studies and no statistically significant data about them. From October 2007 until the present (July 2019), we have continued scientifically rigorous experiments and analyses to detect a so-called "pyramid power". From this, we discovered two unexplained functions of the PS described below.

1) The PS has the function of capturing unconsciousness (force type I) of a human (the test subject) more than 6 km away and converting it into energy detectable by biosensors (1% significance). We hypothesized that there is a positive correlation between the magnitude of the test subject's unconsciousness (force type I) and the magnitude of the energy that the unconsciousness has been converted into by the PS. Furthermore, we hypothesized that there is also a positive correlation between the magnitude of the converted energy and the magnitude of the non-contact effect. As a result of the experiment when the test subject was at home at a distance of 6.55 km from the laboratory, the non-contact effect on the biosensors placed at the PS apex was large in the time period before and after the test subject woke up, and was almost zero at the time of waking up. From this, we found that force type I was time-varying in the time period from the test subject's sleep state to the awake state. We have also been shown that the PS converted time-varying force type I into energy that could be detected by the biosensors without significant time delay. This represented the discovery of the long-distance non-contact effect by the PS function [1, 2].

2) The PS accumulated the influence (force type II) that a human (the test subject) exerted when meditating within the PS. Then the PS converted the influence into an energy detectable by biosensors. With this converted energy, non-contact effects were detected over a long period of several hours to a dozen days after the subject entered the PS and meditated. This represented the discovery of the short-range non-contact effect with delay due to the function of the PS [3-6]. We obtained $p = 3.5 \times 10^{-6}$ (Welch's t-test, two-tails) and the p value was a measure showing the possibility that the difference between the non-contact effect when the test subject was meditating inside the PS, and the non-contact effect when 2 hours had passed after meditation, occurred by chance.

The functions (1) and (2) were both phenomena that appeared because "the PS and a human (the test subject) were related". Also, it was concluded that there are two kinds of force types in a human, force type I and force type II.

In our previous studies, we discovered the functions of the PS that appeared when "the PS and a human were related". Now we have turned our attention to the functions when "the PS and a human were not related". Our purpose in this paper is to verify the existence of the potential power of the PS alone by experiment when "the PS and a human were not related". And our long-term goal is to clarify the characteristics when the potential power of the PS exists.

2. EXPERIMENT AND ANALYSIS METHODS

2.1. Design of the Pyramidal Structure (PS)

The PS used in the experiment is shown in **Figure 1(a)**. The PS was a square pyramid with a height of 107 cm, a ridgeline length of 170 cm and a base length of 188 cm. The angle (tilt angle) between the bottom and the side of the PS was 49.1˚. The base of the PS was raised by four tripods to a height of 73 cm from the floor. The frame of the PS was made of four aluminum pipes (2 cm diameter, 0.36 cm thick pipe wall), the top ends of which were connected. The bottom ends of each pipe were placed at the four corners of a square (188 cm on each side, the base length) made with four aluminum L angles. The four aluminum pipes were not electrically connected to the L angles, and they were not electrically grounded. The four sides of the PS were made of 1 cm thick polystyrene boards, which were not grounded. Each side had a

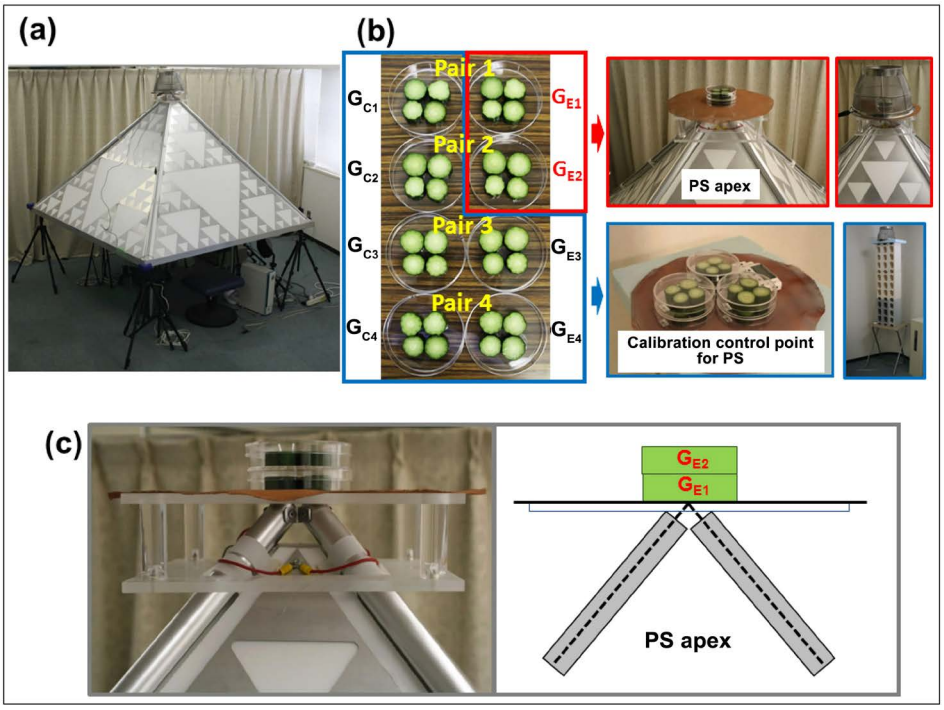

Figure 1. **(a) The pyramidal structure (PS). (b) Left: The biosensors prepared according to the simultaneous calibration technique (SCAT). Right: Photos showing the samples placed at the PS apex and at calibration control point for the PS. (c) Frontal photo and schematic view of the samples placed at the PS apex.**

Sierpinski triangle pattern and it consisted of nine aluminum plates (40.85 cm × 40.85 cm × 43 cm, 0.3 mm thick) which were attached to the polystyrene board. Therefore, a total of 36 aluminum plates were used. The four aluminum pipes were electrically connected to the aluminum plates on all the sides, but since the pipes were not grounded, the aluminum plates were not either. Inside the PS, a transparent acrylic (0.5 cm thick) dome (85 cm diameter, 66.5 cm high) with a spherical shape was placed. The lower portion of the sphere had been removed where the diameter of the sphere cross section was 68.1 cm. The dome was sitting on a wooden square board (99 cm × 99 cm, 3 cm thick) with a 70 cm diameter hole in the center. The bottom surface of the board was held at a height of 85 cm from the floor by four tripods. The center hole in the board allowed the test subject to insert his head and upper body into the dome space. The dome was designed so that the voice of the test subject could resonated when his upper body was in the dome.

2.2. Detection of the "Pyramid Power" (Non-Contact Effect)

In order to clarify the presence of the "pyramid power" in the PS, we verified the non-contact effect on the biosensors (cucumber fruit sections). In general, injuries to living bodies such as plants are known to cause biological protection and repair reactions [7-10]. Regarding these reactions, we noticed that there was a variable gas concentration from a gas generation reaction on the cut section (an injury) of the cucumbers and we analyzed the gas concentration to verify the existence of the "pyramid power" (non-contact effect). To prepare uniform biosensors, we used the simultaneous calibration technique (SCAT) (**Figure 1(b)**) [11]. Researchers at the International Research Institute (IRI) developed the non-contact effect measuring methods based on gas concentration. And using these measurement methods, we successfully detected the healer's non-contact effect and a wave like bio-field around the healer [12-14].

The experimental samples G_{E1} and G_{E2} of Pair1 and Pair2 in **Figure 1(b)** were placed at the PS apex. The control samples G_{C1} and G_{C2} of Pair1 and Pair2 and experimental samples G_{E3}, G_{E4}, and control samples G_{C3} and G_{C4} of Pair3 and Pair4 were placed at the calibration control point 8 m away from the PS. The experimental and control samples were kept in their respective places for 30 minutes. G_E and G_C were the same cut section, but the direction of the cut section was different. The cut section of G_E was in the same direction with respect to the growth axis of the cucumbers, but the cut section of G_C was in the reverse direction. We had previously confirmed experimentally that a difference appeared in the released gas concentration due to the difference in the direction of the cut section, and the gas concentration was $G_E < G_C$ [15, 16].

While the samples were placed at the PS apex and calibration control point, they were electrostatically shielded by an electrically grounded Faraday cage. The Faraday cage was at a height of 180 cm from the floor. At the top of the PS, G_{E1}, G_{E2}, the Faraday cage and a circular copper mesh were put on the PS using insulated support legs (**Figure 1(a)**, **Figure 1(c)**). Under the stacked samples (G_{E1} on the bottom, G_{E2} on the top) there was a circular copper mesh. The circular copper mesh was grounded. The center of the bottom of the Petri dish of G_{E1} and the extended center longitudinal line of the four aluminum pipes of the PS apex coincided (**Figure 1(c)** right). On the other hand, G_{C1} and G_{C2}, G_{E3} and G_{E4}, and G_{C3} and G_{C4} were stacked at the calibration control point in three groups. The larger numbered Petri dish was placed on top for each group. After 30 minutes, the lids of the paired Petri dishes were removed, and each Petri dish was placed in a separate sealed container with a volume of 2.2 liters; the pairs were stored side by side. The storage time was 24 h - 48 h. After storage, the gas concentrations released from the cucumber sections were measured. Gas detection tubes (Ethyl acetate detector tube 141L: Gastech, Japan) and a gas sampling pump (GV-100: Gastech, Japan) were used to measure the gas concentrations.

2.3. Calculation of the Psi Index (ψ) Representing the Magnitude of the Non-Contact Effect

In order to verify the existence of the "pyramid power" for the biosensors placed at the PS apex, in this paper, we introduced the psi index (Ψ), which is an index to quantify the magnitude of the "pyramid power" (non-contact effect). The effect of "pyramid power" can be buried within the noise of the data. The reason is that cucumbers as the biosensors are very sensitive to factors such as individual cucumber differences and environmental conditions. In order to minimize such variables, we adopted a paired sample method (**Figure 1(b)**) where G_E and G_C are paired and compared. The Ψ values are 100 times the natural logarithm of the ratio calculated for the gas concentrations of each pair. The relationship between the J value [17] we have used previously and Ψ was $\Psi = 100J$.

$$\begin{aligned} \Psi_1 &= 100\ln(G_{E1}/G_{C1}), \\ \Psi_2 &= 100\ln(G_{E2}/G_{C2}), \\ \Psi_3 &= 100\ln(G_{E3}/G_{C3}), \\ \Psi_4 &= 100\ln(G_{E4}/G_{C4}). \end{aligned} \quad (1)$$

In Equation (1), G_{E1} to G_{E4} and G_{C1} to G_{C4} were gas concentrations (ppm) measured from the samples as arranged in **Figure 1(b)**. The Ψ_1 to Ψ_4 values were the psi index before calibration. From Ψ_3 and Ψ_4, we thought that the influence due to the difference in the direction of the cut sections of the cucumbers was detected. In addition, we thought that from Ψ_1 and Ψ_2, the result of two influences due to the difference in the direction of the cutting section and the difference in the placement (the PS apex and calibration control point) could be detected. $\Psi_{1(E\text{-}CAL)}$ and $\Psi_{2(E\text{-}CAL)}$ obtained by subtracting the average value of Ψ_3 and Ψ_4 from Ψ_1 and Ψ_2 are results of calibration of various external environment effects such as temperature, humidity, atmospheric pressure, and geomagnetism. Therefore, $\Psi_{1(E\text{-}CAL)}$ and $\Psi_{2(E\text{-}CAL)}$ were considered to reflect only the influence from the PS.

$$\begin{aligned} \Psi_{1(E\text{-}CAL)} &= \Psi_1 - (\Psi_3 + \Psi_4)/2, \\ \Psi_{2(E\text{-}CAL)} &= \Psi_2 - (\Psi_3 + \Psi_4)/2. \end{aligned} \quad (2)$$

Finally, the calibrated psi index at the PS apex was determined by

$$\Psi_{\text{E-CAL}} = (\Psi_{1(\text{E-CAL})} + \Psi_{2(\text{E-CAL})})/2. \quad (3)$$

2.4. Analysis of the Experimental Data

From the results of the earlier experiments that "the PS and a human were related", we found that the PS has a function to capture and convert two force types of a human. From this PS function, we saw two points. 1) A human unconsciousness (force type I) was detected from an experiment several hours before a human (the test subject) entered and meditated inside the PS [1, 2]. 2) When a human (the test subject) entered the PS and meditated, the influence (force type II) was detected for more than ten days [4-6]. In the present paper, we have turned our attention to experimental verification of whether there is a potential power in the PS when "the PS and a human were not related". Therefore, experimental data conducted without the influence of a human's (the test subject's) force type was necessary. We analyzed data obtained from experiments meeting the following three conditions. 1) The experiment was conducted without a human (the test subject) in the PS. 2) The experiment was conducted without a human in the PS for at least 20 days before conducting the experiment. 3) After the experiment, no human was kept inside the PS for at least 48 hours.

3. RESULTS OF THE EXPERIMENT AND ANALYSIS

Figure 2(a) is the distribution of $\Psi_{\text{E-CAL}}$, which represents the magnitude of the non-contact effect calculated from the gas concentration. The vertical axis is $\Psi_{\text{E-CAL}}$, and the horizontal axis is the date. The dates are values from 1 to 366 obtained by starting at 1 and counting from January 1 of each year in which the experiment was conducted. The data analyzed in this paper were obtained from experiments between

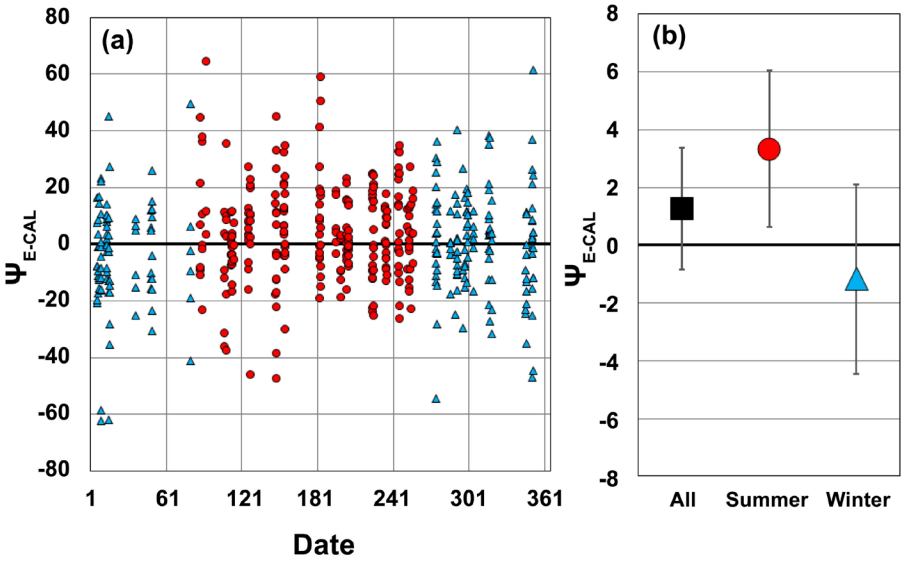

Figure 2. The psi index ($\Psi_{\text{E-CAL}}$) in the case that "the PS and a human were not related". (a) The vertical axis is $\Psi_{\text{E-CAL}}$, and the horizontal axis is the date. The dates are values from 1 to 366 obtained by starting at 1 and counting from January 1 of each year in which the experiment was conducted. The red circles are summer data (n = 252) and the blue triangles are winter data (n = 216). (b) the vertical axis is the $\Psi_{\text{E-CAL}}$ and the horizontal axis shows the average of the data for three groups: all data (black square), summer data (red circle) and winter data (blue triangle). All error bars show 99% confidence interval.

July 2010 and September 2017. For experimental data of the same period, we previously published six papers [1-6] on the function of the PS in which we discovered that "the PS and a human were related" and two papers [15, 16] on the characteristics of the biosensors. The red circles are summer data and the blue triangles are winter data. In **Figure 2(a)** summer data were the results obtained by experiments when the daytime was more than 12 hours. Summer was therefore from the day of the spring equinox to the day of the autumn equinox. The day of the spring equinox when not a leap year was March 20, and the value on the horizontal axis, 81. The day of the autumn equinox when not a leap year was September 23, and the value on the horizontal axis, 267. Analogously, winter data were the results obtained by experiments when the day length was less than 12 hours. The numbers of data were n = 252 for summer data and n = 216 for winter data.

In **Figure 2(b)**, the vertical axis is the $\Psi_{\text{E-CAL}}$, and the horizontal axis shows the three groups of data: all data (black square), summer data (red circle) and winter data (blue triangle). All error bars show 99% confidence interval. The average value of the summer data had 1% significance and the $\Psi_{\text{E-CAL}}$ was a positive value. However, the average value of all data and winter data became zero within the margin of error. This was the result of the experiments conducted when "the PS and a human were not related". Thus, in the summer, the non-contact effect on the biosensors was significant, demonstrating the existence of a potential power of the PS (the "pyramid power"). As a result of analysis of variance (ANOVA), $p = 6.0 \times 10^{-3}$. The p value is a measure showing the possibility that the difference between the average value of the summer data and the winter data may occur by chance (Welch's t-test, two-tails).

From the result of **Figure 2(b)**, the presence of the potential power of the PS was demonstrated (1% significance).

Figure 3 shows the result of calculating the moving average of the $\Psi_{\text{E-CAL}}$. **Figures 3(a)-(c)** are the

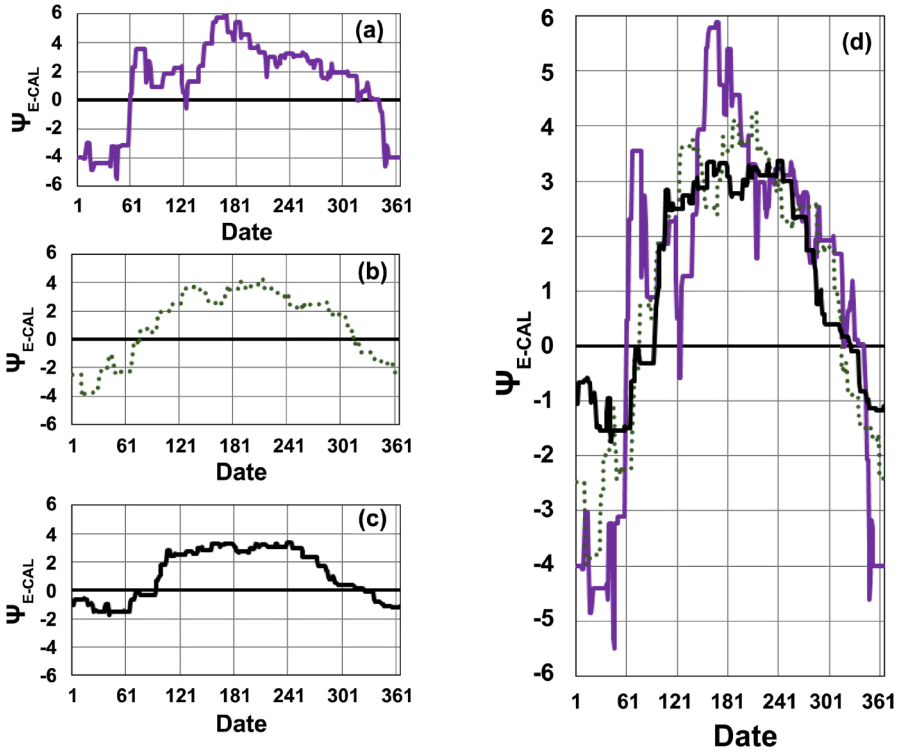

Figure 3. Moving average of $\Psi_{\text{E-CAL}}$. The moving average of $\Psi_{\text{E-CAL}}$ that is shown in Figure 2(a). The sizes of the moving average window are 60 days (a)), 120 days (b)) and 180 days (c)). The vertical axis is $\Psi_{\text{E-CAL}}$, and the horizontal axis is date as explained in the caption of Figure 2(a). (d) is the result of overlapping (a)-(c).

results of moving average when the window size of the $\Psi_{E\text{-}CAL}$ shown in Figure 2(a) is 60 days, 120 days and 180 days, respectively. Figure 3(d) shows the results of overlapping Figures 3(a)-(c). From these results, it became clear that the non-contact effect due to the potential power of the PS was exhibiting a convex shape for the plotted $\Psi_{E\text{-}CAL}$ values in summer. We also found that the potential power of the PS affected the biosensors throughout the year. However, it is difficult to determine if the potential power of the PS is changing continuously throughout the year or if discontinuous changes occur.

From the result of Figure 3, the following two results were demonstrated. 1) The potential power of the PS changed in value between summer and winter. 2) The potential power of the PS (non-contact effect on the biosensors) was larger in summer and smaller in winter.

Figure 4 shows the psi index before calibration. Figure 4(a) shows the moving average of $(\Psi_1 + \Psi_2)/2$, and Figure 4(b) shows the moving average of $(\Psi_3 + \Psi_4)/2$. The moving average window size is 180 days. $(\Psi_1 + \Psi_2)/2$ includes the results of the samples G_{E1} and G_{E2} placed at the PS apex. On the other hand, $(\Psi_3 + \Psi_4)/2$ includes only the results of the samples placed at the calibration control point. The convex shape seen for the plotted summer data in Figure 3(d) appeared prominently in Figure 4(a) but did not appear in Figure 4(b). Therefore, we found that the potential power of the PS detected as a non-contact effect mainly affected the biosensors placed at the PS apex. The correlation coefficient between Figure 4(a) and Figure 4(b) was not a strong correlation, being 0.296.

From the result of Figure 4, it was demonstrated that the potential power of the PS affected only the biosensors placed at the PS apex, and did not affect the biosensors placed at the calibration control point 8 m away from the PS.

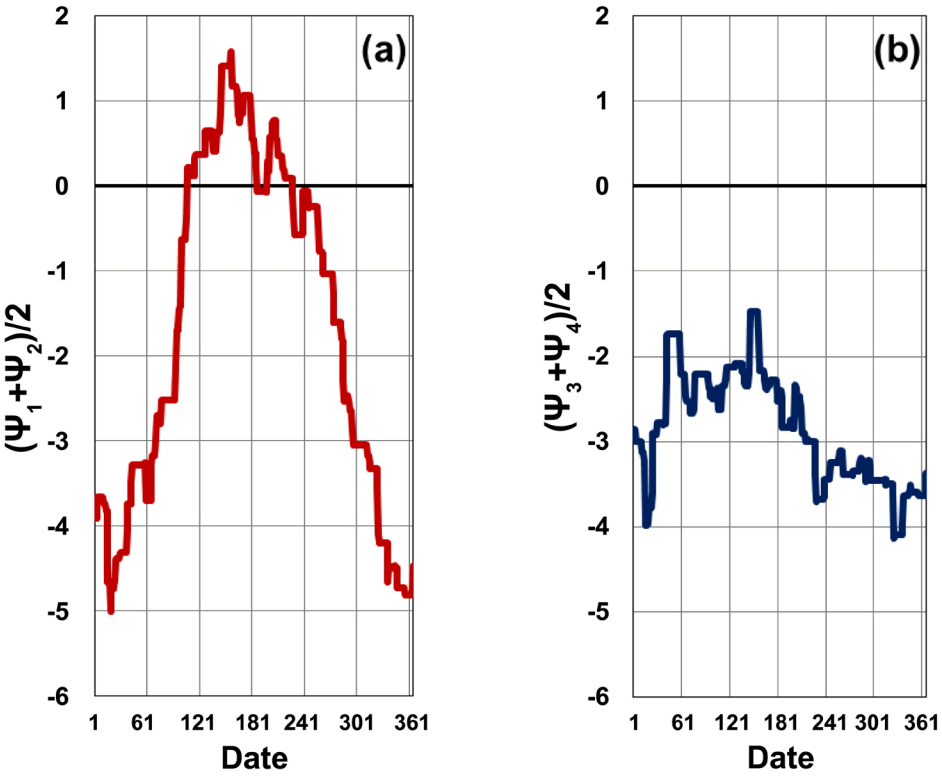

Figure 4. The moving averages of the psi index $(\Psi_1 + \Psi_2)/2$ and $(\Psi_3 + \Psi_4)/2$ before calibration. (a) is the moving average of $(\Psi_1 + \Psi_2)/2$ and (b) is the moving average of $(\Psi_3 + \Psi_4)/2$. The horizontal axis is the date as explained in the caption of Figure 2(a). The moving average window size is 180 days. The correlation coefficient between (a) and (b) is 0.296.

4. DISCUSSION AND CONCLUSION

We conducted experiments to verify the non-contact effect of the PS on biosensors under the condition that "the PS and a human were not related". From them we had three results. 1) The presence of the potential power of the PS was demonstrated with 1% significance (**Figure 2(b)**). 2) The potential power of the PS showed different characteristics in the summer and the winter. We found that the psi index (Ψ), which represents the magnitude of the non-contact effect, tended to increase in the summer and decrease in the winter (**Figure 3**). 3) The potential power of the PS affected only the biosensors placed at the PS apex, and not the biosensors placed at the calibration control point (**Figure 4**). From these results, we concluded that there was a potential power (the "pyramid power" that affected the biosensors) of the PS alone in the case that "the PS and a human were not related". We also concluded that the potential power of the PS varied with the season. This paper is the first report in the world to show this type of effect by scientific measurements.

In order to understand why the non-contact effect due to the potential power of the PS varied with the season, we proposed a hypothesis. First, we discussed the relationship between the potential power of the PS and the gas generation reaction of cucumbers. For this purpose, we considered the change of the psi index before calibration in **Figure 4**. The result of $(\Psi_3 + \Psi_4)/2$, which was not affected by the PS, was considered to be almost constant at negative values throughout the year (**Figure 4(b)**) [16]. On the other hand, $(\Psi_1 + \Psi_2)/2$, which included the results of the samples placed at the PS apex, was larger in summer and smaller in winter than $(\Psi_3 + \Psi_4)/2$ (**Figure 4(a)**). To understand these features, we assumed the following three things. 1) There were two types of potential power (potential power 1 (P_1) and potential power 2 (P_2)) near the PS apex (**Figure 5(a)**). 2) There were at least two types of gas generation reactions

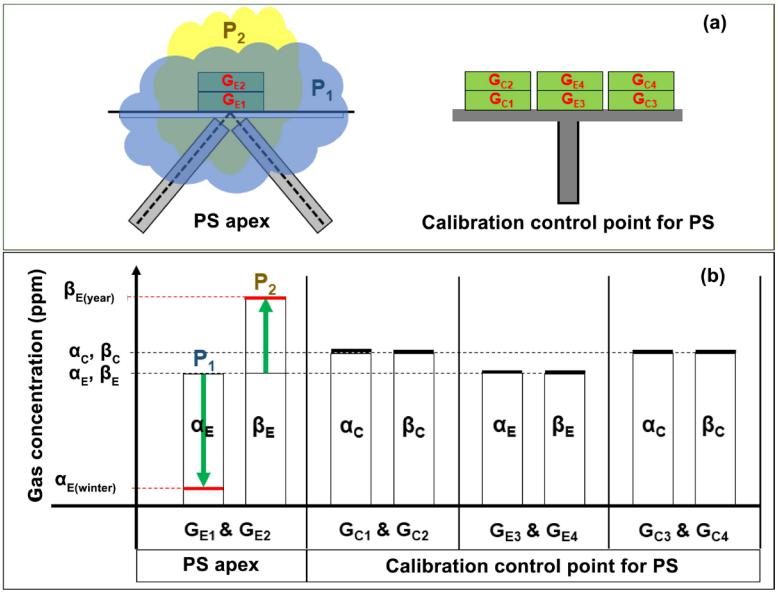

Figure 5. The schematic diagram to consider the seasonal change of potential power of the PS. (a) We hypothesized that two kinds of potential power (P_1, P_2) existed near the PS apex. Samples G_{E1} and G_{E2} placed at the PS apex were affected by P_1 and P_2. (b) We hypothesized two kinds of gas generation reactions of the cucumbers (α reaction, β reaction). α_E, β_E: Average gas concentration generated from experimental samples by α and β reactions. α_C, β_C: Average gas concentration generated from control samples by α and β reactions. From the axial characteristics of the cucumber sections, $\alpha_E < \alpha_C$, $\beta_E < \beta_C$. Here, we assumed that $\alpha_E = \beta_E$ and $\alpha_C = \beta_C$. The α reaction was suppressed by P_1 in the winter, and α_E of G_{E1} & G_{E2} became $\alpha_{E(winter)}$. The β reaction was promoted throughout the year by P_2, and β_E of G_{E1} & G_{E2} became $\beta_{E(year)}$.

of the cucumbers: reaction α and reaction β (**Figure 5(b)**). 3) The samples G_{E1} and G_{E2} placed at the PS apex were affected by the two potential powers P_1 and P_2 of the PS. The α_E and β_E in **Figure 5(b)** were the average gas concentrations generated from the experimental samples by the α reaction and β reaction. Similarly, α_C and β_C were average gas concentrations generated from the control samples. The reason why $\alpha_E < \alpha_C$ and $\beta_E < \beta_C$ in **Figure 5(b)** came from the characteristic that the concentration of released gas differed depending on the difference in the axial direction of the cucumber cut section [15, 16].

Here, in order to facilitate understanding, we assumed $\alpha_E = \beta_E$, $\alpha_C = \beta_C$. At this time, if the following relationship between the potential power of the PS and the gas generation reaction exists, it is possible to understand the results of **Figure 4**: "The α reaction suppresses gas generation in winter by the potential power P_1 of the PS. As a result, α_E of G_{E1} and G_{E2} becomes $\alpha_{E(winter)}$. The β reaction promotes gas generation throughout the year by the potential power P_2 of the PS. As a result, β_E of G_{E1} and G_{E2} becomes $\beta_{E(year)}$." If the results of **Figure 4(a)** and **Figure 4(b)** can be derived from the relationship between the potential power of the PS and the gas generation reaction, it can be understood that the change of non-contact effect ($\Psi_{E\text{-}CAL}$) in **Figure 3** is caused by the potential power of the PS.

We experimentally demonstrated the existence of the potential power of the PS and some of its properties. This opens up the possibility that the so-called "pyramid power", which has often been recognized as having no scientific basis, may become a new field of science. The issues to be further investigated are changing the experimental variables such as the structural parameters of the PS (e.g., size, material and the fractal patterns). So many issues remain to be studied. In the future, we may expect to see developments in many fields applying the "pyramid power".

A part of this research was done under the Sakamoto Hyper-tech Project (SHyP, October 2007 to September 2017) as a joint activity between Aquavision Academy Co., Ltd. (President: Masamichi Sakamoto) and the International Research Institute (IRI, Chairman of the Board of Directors: Mikio Yamamoto).

CONFLICTS OF INTEREST

The authors declare no conflicts of interest regarding the publication of this paper.

REFERENCES

1. Takagi, O., Sakamoto, M., Yoichi, H., Kokubo, H., Kawano, K. and Yamamoto, M. (2019) Discovery of an Unexplained Long-Distance Effect Caused by the Association between a Pyramidal Structure and Human Unconsciousness. *Journal of International Society of Life Information Science*, **37**, 4-16.
2. Takagi, O., Sakamoto, M., Yoichi, H., Kokubo, H., Kawano, K. and Yamamoto, M. (2019) Discovery from the Experiment on the Unexplained Functions of the Pyramidal Structure—The Phenomenon Caused by the Personal Relationship. *Journal of International Society of Life Information Science*, **37**, 60-65.
3. Takagi, O., Sakamoto, M., Kokubo, H., Yoichi, H., Kawano, K. and Yamamoto, M. (2013) Meditator's Non-Contact Effect on Cucumbers. *International Journal of Physical Sciences*, **8**, 647-651. https://doi.org/10.5897/IJPS2012.3800
4. Takagi, O., Sakamoto, M., Yoichi, H., Kokubo, H., Kawano, K. and Yamamoto, M. (2015) Discovery of an Anomalous Non-Contact Effect with a Pyramidal Structure. *International Journal of Sciences*, **4**, 42-51. https://doi.org/10.18483/ijSci.714
5. Takagi, O., Sakamoto, M., Yoichi, H., Kokubo, H., Kawano, K. and Yamamoto, M. (2016) An Unknown Force Awakened by a Pyramidal Structure. *International Journal of Sciences*, **5**, 45-56. https://doi.org/10.18483/ijSci.1038
6. Takagi, O., Sakamoto, M., Yoichi, H., Kokubo, H., Kawano, K. and Yamamoto, M. (2016) Necessary Condition of an Anomalous Phenomenon Discovered by a Pyramidal Structure. *Journal of International Society of Life*

Information Science, **34**, 154-157.

7. Farmer, E.E. (2013) Surface-to-Air Signals. *Nature*, **411**, 854-856. https://doi.org/10.1038/35081189
8. Ozawa, R., Arimura, G., Takabayashi, J., Shimoda, T. and Nishioka, T. (2000) Involvement of Jasmonate- and Salicylate-Related Signaling Pathways for the Production of Specific Herbivore-Induced Volatiles in Plants. *Plant and Cell Physiology*, **41**, 391-398. https://doi.org/10.1093/pcp/41.4.391
9. De Moraes, C.M., Lewis, W.J., Paré, P.W., Alborn, H.T. and Tumlinson, J.H. (1998) Herbivore-Infested Plants Selectively Attract Parasitoids. *Nature*, **393**, 570-573. https://doi.org/10.1038/31219
10. De Moraes, C.M., Mescher, M.C. and Tumlinson, J.H. (2001) Caterpillar-Induced Nocturnal Plant Volatiles Repel Conspecific Females. *Nature*, **410**, 577-580. https://doi.org/10.1038/35069058
11. Kokubo, H., Takagi, O. and Koyama, S. (2010) Application of a Gas Measurement Method—Measurement of Ki Fields and Non-Contact Healing. *Journal of International Society of Life Information Science*, **28**, 95-103.
12. Kokubo, H. and Yamamoto, M. (2009) Controlled Healing Power and Ways of Non-Contact Healing. *Journal of International Society of Life Information Science*, **27**, 90-105.
13. Kokubo, H., Takagi, O., Koyama, S. and Yamamoto, M. (2011) Discussion of an Approximated Equation for Special Distribution of Controlled Healing Power around a Human Body. *Journal of International Society of Life Information Science*, **29**, 23-34. https://doi.org/10.5136/lifesupport.23.29
14. Kokubo, H. (2015) Ki or Psi—Anomalous Remote Effects of Mind-Body System. Nova Science Publishers, Inc., New York.
15. Takagi, O., Sakamoto, M., Yoichi, H., Kokubo, H., Kawano, K. and Yamamoto, M. (2018) Discovery of Seasonal Dependence of Bio-Reaction Rhythm with Cucumbers. *International Journal of Science and Research Methodology*, **9**, 163-175.
16. Takagi, O., Sakamoto, M., Yoichi, H., Kokubo, H., Kawano, K. and Yamamoto, M. (2018) Relationship between Gas Concentration Emitted from Cut Cucumber Cross Sections and Growth Axis. *International Journal of Science and Research Methodology*, **9**, 153-167.
17. Kokubo, H., Takagi, O. and Yamamoto, M. (2009) Development of a Gas Measurement Method with Cucumber as a Bio-Sensor. *Journal of International Society of Life Information Science*, **27**, 200-213.